

Manipulation of coherent atom waves using accelerated two-dimensional optical lattices

Wei-Chih Ting, Dian-Jiun Han, and Shin-Tza Wu

Department of Physics, National Chung Cheng University, Chiayi 621, Taiwan

E-mail: phystw@gmail.com

Abstract. We study the dynamics of Bose-Einstein condensates in accelerated two-dimensional optical square lattices by numerically solving the Gross-Pitaevskii equation. We consider the regime with negligible mean-field interactions and examine in detail the pulses of atom clouds ejected from the condensate due to Landau-Zener tunnelling. The pulses exhibit patterned structures that can be understood from the momentum-space dynamics of the condensate. Aside from conceiving realization of a pulsed two-dimensional atom laser, we demonstrate that, by exploring the band structure of the lattice, Landau-Zener tunnelling and Bragg reflection of the condensate inside the optical lattice can provide means for manipulation of coherent atom waves.

1. Introduction

The past two decades have witnessed the fruitful interplay between condensed matter physics and ultracold atom physics. While cold atom systems have provided new arena for condensed matter physics, at the same time, concepts and ideas from condensed matter physics have opened up new directions for cold atom physics. For instance, by loading ultracold atoms into optical potentials due to standing laser waves (i.e. optical lattices), it is possible not only to build up “quantum simulators” for condensed matter systems (see, for example, [1]), but also to control and manipulate cold atoms utilizing concepts from traditional solid-state systems (see, for instance, [2]). In this work, we wish to further explore the latter lines of investigation.

Electrons in solids are subject to periodic potentials due to the array of ion cores that constitutes the lattice. In ideal situations, the electron eigenfunctions take the form of a particular structure that is called the Bloch wave, and the corresponding eigen-energies cluster into energy bands that are separated by energy gaps (see e.g. [3]). As a consequence, electrons in solids can behave quite differently compared with those in free space. For instance, when a weak uniform static electric field is applied to the solid, instead of being uniformly accelerated, the electrons would carry out oscillatory motions (the Bloch oscillation; see e.g. [4]). This oscillatory motion can be understood as Bragg reflections of the Bloch states in momentum space (or \mathbf{k} -space) at regions where energy gaps occur. If the bias field is large, the electrons can gain sufficient energy that would lead to finite probability for tunnelling across the energy gaps, resulting in transitions to higher energy bands (the Landau-Zener tunnelling; see, for example, [4]). In this work, we wish to consider the cold atom counterpart of the above construction. Namely, we shall consider a cloud of Bose-Einstein condensate subject to a periodic potential due to standing laser waves that form an optical lattice. We shall examine dynamics of the condensate under the action of an external bias that corresponds to the uniform static electric field above. Experimentally this bias can be furnished in a number of ways: one could make use of direct gravity pull on the atoms, or introduce time-dependent frequency shifts between the lattice beams so that an effective acceleration on the atoms occurs (see e.g. [5, 6]). For spin polarized condensates, it is also possible to generate the acceleration by means of magnetic field gradients [7].

The dynamics of ultracold atoms in one-dimensional (1D) optical lattices subject to uniform accelerations have been investigated extensively [2]. In addition to the observation of Bloch oscillations [8], Wannier-Stark ladders [9], and Landau-Zener tunnelling [10] for condensates in accelerated 1D optical lattices, possible realizations for 1D “atom laser” have also been achieved [11] using such systems.‡ By loading Bose condensed ^{87}Rb atoms into a vertical 1D optical lattice, Anderson and Kasevich have demonstrated that for appropriate lattice strengths, pulses of atom clouds can tunnel out of the optical lattice due to the gravity pull. The generation of pulses of coherent

‡ For other realizations of atom lasers (involving and not involving accelerated optical lattices), see e.g. [7] and references therein.

atom waves thus suggests the system being an 1D pulsed atom laser [11, 12]. For two-dimensional (2D) systems, there have also been studies of Bloch oscillations, Landau-Zener tunnelling (at lower energy bands; cf. below) [13, 14], and Bloch-Zener oscillations [15] of ultracold atoms in accelerated 2D optical lattices.§ The richer dynamics of the condensates in 2D lattices has been proposed to be possible means for manipulation of the coherent atom waves [13, 14, 15]. Along these lines of investigation, we shall examine in this work the Landau-Zener tunnelling of atom waves within 2D optical lattices. More specifically, we will be interested in physical configurations similar to the 1D system considered by Anderson and Kasevich [11, 12]. To simplify the analysis, however, we will focus in this work on regimes where the nonlinear mean-field interaction is negligible (cf. [11, 12]). Effects of the mean-field interaction in related problems are investigated in [20, 21].

In order to conceive a 2D atom laser, we shall consider a condensate loaded into a uniformly accelerated 2D optical square lattice in the regime where Landau-Zener tunnelling is the predominant effect. In particular, since the atoms need to tunnel out of the lattice to form the lasing pulses, dynamics of the condensate at higher energy bands will be essential (cf. [13, 14]). As we will see below the more complicated energy landscape at higher energy bands turns out to enrich the structure for the output pulses of the atom laser. We shall study the dynamics of the condensate by numerically solving the Gross-Pitaevskii (GP) equation (see e.g. [6]). For appropriate accelerations we shall find pulses of atom clouds tunnelling out of the condensate, which manifest a patterned structure. We will show that these are consequences of Bragg reflection and Landau-Zener tunnelling at higher energy bands. For energy states in these higher energy bands, unlike their 1D counterparts [11], characteristics of Bloch waves still manifests in the atom waves; even though they are quite close to free-particle states. By means of \mathbf{k} -space analysis, we shall relate propagation of the coherent atom waves in real space to the \mathbf{k} -space dynamics of the condensate. As we will soon recognize, aside from a 2D atom laser with patterned pulses, our result can help envisage beam splitters for coherent atom waves.

In the following, we shall start in section 2.1 with an introduction to our theoretical formulation. Numerical results for our simulations will then be presented in section 2.2. In section 2.3 we will try to understand these results base on \mathbf{k} -space dynamics of the condensate. We will then demonstrate in section 3 how this analysis can help provide a useful tool for manipulation of coherent atom waves. A brief conclusion is supplied at the end of the article.

§ There have also been related theoretical and experimental studies in photonic crystals [16, 17, 18, 19].

2. Two-dimensional atom laser

2.1. Theoretical formulation

Let us consider a Bose-Einstein condensate of atoms with atomic mass m in a two dimensional optical lattice [22]. We shall look into the regime where the low temperature ground-state dynamics of the condensate can be described by the GP equation (see e.g. [6])

$$i\hbar\frac{\partial}{\partial t}\Psi(\boldsymbol{\rho}, t) = \left(-\frac{\hbar^2}{2m}\nabla_{\boldsymbol{\rho}}^2 + V_{ext}(\boldsymbol{\rho}, t) + U|\Psi(\boldsymbol{\rho}, t)|^2\right)\Psi(\boldsymbol{\rho}, t), \quad (1)$$

where Ψ is the condensate wave function, $\boldsymbol{\rho} = (x, y)$ is the 2D position vector, $\nabla_{\boldsymbol{\rho}}^2 \equiv \left(\frac{\partial^2}{\partial x^2} + \frac{\partial^2}{\partial y^2}\right)$ is the 2D Laplacian operator, V_{ext} is the total external potential acting on the condensate, and U is the mean-field coupling constant. In order to examine dynamics of the condensate in an accelerated optical lattice, here the external potential V_{ext} consists of two parts: one due to the optical lattice, and the other from a uniform acceleration. The optical lattice potential that we shall consider is similar to that in [22]

$$V_{opt}(x, y) = V_0 [\cos^2(q_x x) + \cos^2(q_y y)] , \quad (2)$$

where V_0 is a real constant, q_x, q_y are wave numbers for the laser beams that build up the optical lattice. In experiments the lattice beams usually have the same wavelength, so that $q_x = q_y = q$. We shall thus consider this case, so that (2) corresponds to a 2D square lattice with lattice constant $a = \pi/q$. If the lattice is uniformly accelerated with acceleration \mathbf{g} , there would be the corresponding potential

$$V_g(x, y) = -m\mathbf{g}\cdot\boldsymbol{\rho}. \quad (3)$$

In order to maintain the phase coherence of the atom laser that we have in mind, it is crucial to avoid large potential strengths [12]. This is because for high lattice strength V_0 , if one regards the condensate as a collection of individual atom clouds over the lattice sites, with increasing V_0 the wave function overlap between neighbouring sites would drop and, at the same time, the mean-field interaction $U|\Psi|^2$ would grow due to the more localized wave function and stronger coupling U [23]. These effects combine to reduce the phase coherence among the condensates on different lattice sites [12, 24]. This can be understood as a consequence of the number-squeezing of the condensate on each lattice site due to the mean-field interaction when V_0 is large, which enhances the (uncorrelated) phase fluctuations among the lattice sites [24]. It is essential to recognize the role of the mean-field interaction in this decoherence mechanism: with $U = 0$, as long as the wave function overlap between adjacent sites remains finite, there would not be any decoherence even for large V_0 . We will thus be interested in the regime where the mean-field interaction $U|\Psi|^2$ in (1) is negligible compared with the strength of the optical potential.|| In experiments, this would correspond to the cases

|| Since the mean-field interaction is proportional to the (s -wave) scattering length and the density of

where well-resolved Bragg peaks can be visible when the condensate is released from the optical lattice [24, 25] (notice, however, the caveat pointed out by [28]); namely the system is supposed to be deep on the “superfluid” side of the phase diagram. This would at the same time also justify our analysis of the condensate dynamics based on the GP equation, since for large potential strengths the system could make transitions into the Mott insulating phase [25]. Throughout this work, we will therefore consider the following GP equation

$$i\hbar \frac{\partial \Psi}{\partial t} = \left(-\frac{\hbar^2}{2m} \nabla_{\rho}^2 + V_0 [\cos^2(qx) + \cos^2(qy)] - m\mathbf{g} \cdot \boldsymbol{\rho} \right) \Psi. \quad (4)$$

The time evolution of the condensate can then be analyzed reliably using the Crank-Nicholson method [29], which we shall now turn to.

2.2. Atom laser

Let us suppose we have initially in free space a stationary condensate which has a Gaussian wave function

$$\Psi(\rho, t_0) = \sqrt{\frac{N}{2\pi\sigma^2}} \exp\left(-\frac{\rho^2}{4\sigma^2}\right), \quad (5)$$

where N is the total number of atoms, $\rho = (x^2 + y^2)^{1/2}$, and σ is the width of the wave packet. In order to transfer the condensate into the lattice ground state, without turning on V_g , the Gaussian wave packet is first subject to the optical lattice potential V_{opt} and set to evolve for a period of time. At time $t = 0$, we switch on V_g [see (3)] so that a static uniform acceleration \mathbf{g} starts acting on the condensate. It is then our main purpose to examine the subsequent dynamics of the condensate. As explicated previously, to avoid complications from strong lattice potentials we restrict here to potential strengths of order of the recoil energy

$$E_R \equiv \frac{\hbar^2 q^2}{2m} = \frac{h^2}{8ma^2}. \quad (6)$$

We carry out numerical simulations for the above procedures base on the GP equation (4). The results for two different accelerations are presented in figure 1, where we have used $\sigma = 2.5a$ and $N = 2\pi\sigma^2$ for the initial wave function (5), and $V_0 = 1.0E_R$ for the optical potential (2). The acceleration is set to have the magnitude $g = \frac{\pi E_R}{4ma}$, which has been chosen somewhat arbitrarily; one only has to make sure that it would lead to appreciable tunnelling probability for the condensate (see later). For convenience, we use the following time scale for the time evolution of the condensate

$$T_B = \frac{\left(\frac{2\pi}{a}\right)}{\left(\frac{mg}{\hbar}\right)} = \frac{h}{mga} = \frac{1}{g} \sqrt{\frac{8E_R}{m}}, \quad (7)$$

which is the time for a Bloch state to cross one complete Brillouin zone (namely, the Josephson time [11], or the Bloch period [14]) when \mathbf{g} is along the lattice (1,0)

the condensate, besides tuning the lattice strength V_0 (such as in [11, 12, 24, 25]), experimentally one could also attain this regime by using condensates with low densities and/or reducing the scattering length via Feshbach resonances [26, 27].

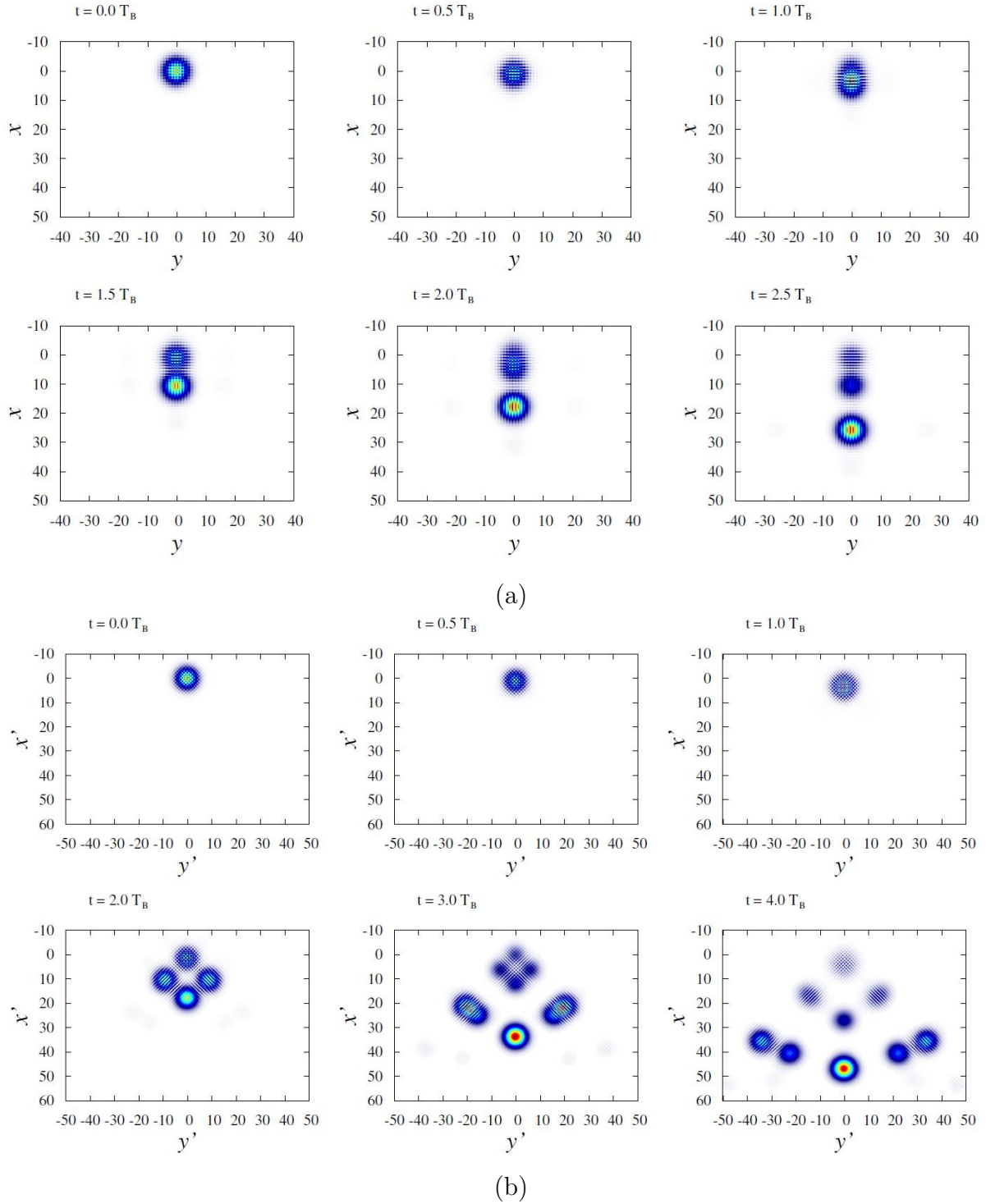


Figure 1. Numerical results for accelerated condensates in a 2D square lattice with the acceleration \mathbf{g} along (a) the $(1,0)$ direction and (b) the $(1,1)$ direction. For both cases we have $V_0 = 1.0E_R$ and $g = \frac{\pi E_R}{4 ma}$, and the time scale T_B is given by (7). Notice that in (b), for convenience, the plots are made with respect to the coordinates $x' = (x + y)/\sqrt{2}$, $y' = (y - x)/\sqrt{2}$, so that \mathbf{g} points along the x' -axis. In all plots the coordinates are measured in units of the lattice constant a .

direction. ¶ We shall henceforth adopt a coordinate system with x -axis along the lattice $(1, 0)$ direction, and y -axis the $(0, 1)$ direction.

As shown in figure 1(a), for \mathbf{g} along the $(1, 0)$ direction pulses of atom clouds tunnel out of the condensate in a manner reminiscent of that in accelerated 1D optical lattices [11, 12]. The sequence of pulses generated are equally spaced in time by T_B and aligned entirely in the $(1, 0)$ direction. For \mathbf{g} along the $(1, 1)$ direction [see figure 1(b)], however, the pulses have a more complicated structure. There are initially three pulses generated from the condensate in three different directions which subsequently split into further sub-pulses. Clearly, this immediately brings up interesting possibilities for applications: besides a “patterned” atom laser, one could also use the 2D optical lattice as a beam splitter for coherent atom waves, as we will soon demonstrate. In the following we shall first examine the origin of this pattern and afterwards elaborate on its possible applications.

2.3. \mathbf{k} -space dynamics

We shall now attempt to understand the results above from the viewpoint of \mathbf{k} -space dynamics of the condensate. This analysis will turn out very useful for real-space manipulations of atom waves using accelerated 2D optical lattices.

In the absence of lattice acceleration (i.e. $g = 0$), the eigenstates of the GP equation (4) for the condensate are the Bloch states (see e.g. [3]). Each Bloch state is characterized by the quantum numbers \mathbf{k} (the Bloch wave-vector) and n (the band index). For the initial wave function (5), it corresponds in \mathbf{k} -space to a Gaussian centering at $\mathbf{k} = (0, 0)$ with a spread $\delta k_x = \delta k_y = (2\sigma)^{-1}$. Therefore, the subsequent time evolution of the condensate would yield wave packets that are superpositions of Bloch states with width $\delta k \sim (2\sigma)^{-1}$. For the simulations in figure 1 we have $\sigma = 2.5a$, thus in \mathbf{k} -space, instead of a single point, each atom cloud corresponds to a wave packet that spreads around a central value with area $\pi(\delta k)^2 \sim \frac{\pi}{4\sigma^2} = \frac{\pi}{25a^2}$, which is $\frac{1}{100\pi} \simeq 0.32\%$ the area of one single Brillouin zone. In the analysis below, we shall ignore the spread in \mathbf{k} and focus on the center of each wave packet, as if the atom cloud were in a sharp Bloch state characterized by a single Bloch wave vector. In a more quantitative treatment, one can take into account the spreading by averaging over the distribution of the Bloch wave vectors [8].

In view of the above, the motion of the condensate under the action of a uniform static acceleration \mathbf{g} can then be dealt with using a semiclassical approach. Within each band (namely, for one specific n) the dynamics of the condensate follows the equations of motion (see e.g. [3])

$$\frac{d\boldsymbol{\rho}}{dt} = \frac{1}{\hbar} \nabla_{\mathbf{k}} E_n, \quad (8)$$

¶ Notice that for \mathbf{g} along arbitrary directions, T_B would be in general not identical to the period for the Bloch oscillation. In fact, it is possible to have open trajectories for Bloch oscillations [14]. In this case, the Bloch period does not exist.

$$\hbar \frac{d\mathbf{k}}{dt} = m\mathbf{g}, \quad (9)$$

where $\boldsymbol{\rho}$ is, as before, the 2D position vector, and E_n is the eigenenergy for the Bloch state. As is clear from (9), under the action of a constant acceleration \mathbf{g} the Bloch state would proceed steadily in \mathbf{k} -space along the direction determined by \mathbf{g} . However, when the state arrives at zone boundaries where energy gaps exist, the state would have to either make transitions to higher energy bands (Landau-Zener tunnelling) or be reflected to other regions of the same zone (Bragg reflection), so that it could continue its course of evolution according to (9). Notice that these processes are not included in (9) since two or more energy bands can be involved. When only two states are involved, one can find that the tunnelling probability would be (see e.g. [4])

$$P = \exp\left(-\frac{\pi^2}{4} \frac{E_{gap}^2}{mgaE_0}\right), \quad (10)$$

where E_{gap} is the energy gap at the \mathbf{k} -point in question, and E_0 is the corresponding free-particle energy. If the acceleration g is small, the tunnelling probability would be exponentially small. The state would then be Bragg reflected to another state within the original zone, and subsequently continue to evolve in accordance with (8), (9) until it meets another zone boundary. If the state has low probability for interband transitions, its motion would be limited to a single zone and the motion would be oscillatory in both real and \mathbf{k} spaces (which is the Bloch oscillation) [14]. However, for larger values of g the tunnelling probability can become appreciable. The state can then tunnel into higher energy bands and give rise to pulses of atom clouds in real space moving with group velocities determined by (8). As we will find out soon, the patterns of the atom pulses in figure 1 are consequences of Bragg reflection and Landau-Zener tunnelling of the atom waves. Base on this observation we will explain below, how this picture can be used to carry out coherent manipulations of atom waves.

On the grounds of the foregoing analysis, we note that the state of the condensate migrates over the \mathbf{k} -space under the pull of \mathbf{g} and hops around via Bragg reflections. It is thus very helpful to examine the \mathbf{k} -space dynamics of the condensate using the extended-zone picture (see e.g. [4]). Figure 2 shows the extended-zone energy landscape over \mathbf{k} -space obtained from direct diagonalization for the condensate in the 2D square lattice (2). Energy gaps exist at regions where there are discontinuities in the energy contours, which appear as dark shading lines in figure 2(b); the darker the shading is, the larger the energy gap is. Notice that not every zone boundary has energy gaps. As in the extended-zone scheme the zone index is identical to the band index, we shall henceforth use them interchangeably.

In our simulations in figure 1, we have chosen $g = \frac{\pi}{4} \frac{E_R}{ma}$, which is sufficiently large to ensure that the tunnelling probability out of the first band is always appreciable for $V_0 = 1.0E_R$. With the initial wave function (5), the condensate starts at $t = 0$ from the state $\mathbf{k} = (0, 0)$ in the first zone. For figure 1(a) the acceleration points along the $(1, 0)$ direction, therefore according to (9) the condensate would proceed along the k_x -axis until it meets the zone boundary at $k_x = \frac{\pi}{a}$. The wave packet then becomes partly

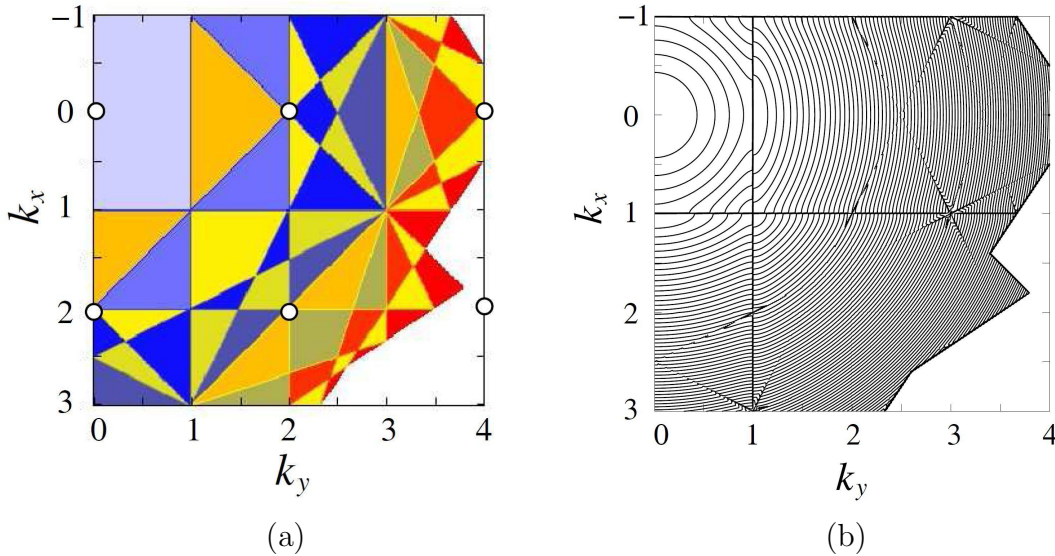


Figure 2. (a) The first twelve Brillouin zones for the 2D square lattice in the extended-zone scheme. The open circles represent reciprocal lattice points. (b) shows contours for the corresponding energy landscape when $V_0 = 1.0E_R$. Here k_x, k_y are both in units of π/a . For regions not shown here, one can infer the zone structure and energy landscape up to the twelfth zone from symmetry of the lattice.

reflected back to the first zone and partly transmitted into the second zone, giving rise to the first tunnelling pulse shown in figure 1(a). The pulse that enters the second zone proceeds again according to (9) until it meets the zone boundary at $\mathbf{k} = (\frac{2\pi}{a}, 0)$, where three Bragg planes intersect. From figure 2(b) it is clear that the energy gap at this point is tiny, thus the pulse can tunnel through entirely. As the wave packet moves along, its energy also grows. Eventually the wave packet becomes essentially free, since it can overcome any energy gap that it encounters [see (10)]. Notice that this result is essentially identical to that for 1D optical lattices [11, 12].

For acceleration along the (1, 1) direction [see figure 1(b)], the \mathbf{k} -space dynamics for the condensate becomes more complicated. Again, the condensate starts at $t = 0$ from the state $\mathbf{k} = (0, 0)$ and evolves initially according to (9) along the (1, 1) direction. However, at $t = T_B/\sqrt{2}$ the state reaches the point $\mathbf{k} = (\frac{\pi}{a}, \frac{\pi}{a})$, where bands 1 – 4 meet. Due to the large energy gap, the condensate can have a partial wave Bragg reflected back into the first band [to the point $\mathbf{k} = (-\frac{\pi}{a}, -\frac{\pi}{a})$] and a partial wave tunnelling into the second band [or the third band, since they are degenerate at this point; see figure 2(b)]. For the partial wave entering into the second band, nevertheless, since the acceleration \mathbf{g} would drive the system to evolve along the (1, 1) direction, the state has to either tunnel immediately into the fourth band, or be Bragg reflected within band 2. The four atom clouds visible at $t = 2.0T_B$ in figure 1(b) represent each of the above possibilities: the atom cloud at the top corner is the partial wave that is Bragg reflected back into the first band, executing an oscillatory motion in both real and \mathbf{k} -spaces; the lower one

is the partial wave that tunnels directly into the fourth band. The two side pulses are partial waves that are Bragg reflected to the points $\mathbf{k} = (\pm \frac{\pi}{a}, \mp \frac{\pi}{a})$ which subsequently evolve under the acceleration \mathbf{g} towards the states $(\frac{2\pi}{a}, 0)$ and $(0, \frac{2\pi}{a})$, respectively. For the three partial waves that tunnel out of the first band, the acceleration \mathbf{g} continues to bring them forward along the (1, 1) direction. The central pulse becomes essentially free, as there is no longer any appreciable energy gap along its \mathbf{k} -space trajectory. For the two side pulses, however, as one can see from figure 2(b) there remain several gaps that they shall cross.

Since the two side pulses are symmetric, it will suffice to focus our analysis on one of them. Let us consider the one on the right. After being Bragg reflected to the point $(-\frac{\pi}{a}, \frac{\pi}{a})$, the pulse evolves under the pull of \mathbf{g} along the (1, 1) direction. It will therefore come across an energy gap at $\mathbf{k} = (\frac{\pi}{3a}, \frac{7\pi}{3a})$ at the time $t = \frac{7\sqrt{2}}{6} T_B \simeq 1.650 T_B$. For the result in figure 1(b), one can rule out any possibility for Bragg reflection at this point since the sub-pulses become visible only at $t = 2.0 \sim 3.0 T_B$ (for a more detailed check, see later). The next energy gap that the pulse would meet occurs at $t = \frac{3}{\sqrt{2}} T_B \simeq 2.121 T_B$ at the point $\mathbf{k} = (\frac{\pi}{a}, \frac{3\pi}{a})$. As we shall explain in greater detail below, at this point the pulse turns out to be partially Bragg reflected to the state $\mathbf{k} = (-\frac{\pi}{a}, \frac{3\pi}{a})$ and partially tunnels forward along its original trajectory. Therefore, the original pulse is split into two sub-pulses, resulting in the final pattern seen in figure 1(b).

To substantiate the arguments in the preceding paragraph, one could consider an arbitrary Bloch state on the line segment between the \mathbf{k} points $(-\frac{\pi}{a}, \frac{\pi}{a})$ and $(\frac{\pi}{3a}, \frac{7\pi}{3a})$, and apply to the state the same acceleration \mathbf{g} as above, but now in a *controlled* manner. For instance, starting from the point $\mathbf{k} = (-\frac{\pi}{2a}, \frac{3\pi}{2a})$, we apply the acceleration \mathbf{g} for the duration $\Delta t = 1.0 T_B$ and then turn it off. This would send the pulse to the state $\mathbf{k} = (\frac{-1+2\sqrt{2}}{2} \frac{\pi}{a}, \frac{3+2\sqrt{2}}{2} \frac{\pi}{a}) \simeq (\frac{0.914\pi}{a}, \frac{2.914\pi}{a})$, which lies between the points $(\frac{\pi}{3a}, \frac{7\pi}{3a})$ and $(\frac{\pi}{a}, \frac{3\pi}{a})$, and then leave it to evolve freely under the lattice potential (2). We find that in this case the atom cloud remains a single one throughout its time evolution. If now the acceleration is kept on for a longer period of time, so that the pulse could go beyond the point $\mathbf{k} = (\frac{\pi}{a}, \frac{3\pi}{a})$ slightly, one would observe that the two sub-pulses are generated. To confirm that Bragg reflection and Landau-Zener tunnelling do occur at $(\frac{\pi}{a}, \frac{3\pi}{a})$, one could repeat the above procedures but apply now a reduced acceleration along (1, 1) direction, say, $g' = \frac{\pi}{20} \frac{E_R}{ma}$. One would find in this case only one single pulse appears, even though an acceleration duration that could have sent the state beyond $\mathbf{k} = (\frac{\pi}{a}, \frac{3\pi}{a})$ had been applied. What happens here is that the pulse is Bragg reflected from $(\frac{\pi}{a}, \frac{3\pi}{a})$ to the state $(-\frac{\pi}{a}, \frac{3\pi}{a})$, and then tunnels into the next band under the action of \mathbf{g}' .⁺ To further endorse our argument, we notice that the directions of the group velocities of the wave packets, according to (8), can be read off from the contours in figure 2(b). Hence the sub-pulse that tunnels through from $\mathbf{k} = (-\frac{\pi}{a}, \frac{3\pi}{a})$ has a group velocity almost parallel

⁺ There are in fact other possible final states for the Bragg reflection [3]. However, they are suppressed here since the optical potential (2) has Fourier components only for $\Delta\mathbf{k} = (0, 0), (\pm 2\pi/a, 0),$ and $(0, \pm 2\pi/a)$.

to the $(0, 1)$ direction, while the one that tunnels forward from $\mathbf{k} = (\frac{\pi}{a}, \frac{3\pi}{a})$ would be more free-particle like [i.e. its real space trajectory would bend downwards just like a projectile; see figure 1(b)]. From the perspective of energetics, we notice that along the $(1, 1)$ direction, tunnelling across the point $(-\frac{\pi}{a}, \frac{3\pi}{a})$ would send the wave packet into the ninth band (degenerate with the tenth band), while across $(\frac{\pi}{a}, \frac{3\pi}{a})$ would bring it into the eleventh band (degenerate with the twelfth band). Taking into account the finite width of the wave packet, one can find that the former option is evidently energetically more favourable. It is also possible to confirm our argument base on Fourier analysis of the atom clouds [30].

Although a more quantitative analysis of the problem than that presented above is possible [17], our approach in the foregoing paragraph has its merits. Besides providing a check for our argument it also alludes to one important point: in addition to considering condensates with zero (center-of-mass) initial velocity (as was done for the simulations in figure 1), one could also consider an initial wave function with non-zero wave vector. Our analysis thus brings out a useful means for the manipulation of coherent atom waves, as we shall now explain.

3. Manipulation of coherent atom waves

In order to prepare a condensate with non-zero Bloch wave vector \mathbf{k}_0 , one can start from a stationary wave packet with the wave function (5). Without turning on the optical lattice potential, one applies first an acceleration \mathbf{g}_0 (along the \mathbf{k}_0 direction) to the stationary condensate for the period of time $\Delta t = \frac{\hbar k_0}{m g_0}$ and then switch it off. The condensate would now have acquired the designated wave vector \mathbf{k}_0 and the wave function would be

$$\Psi(\boldsymbol{\rho}) = \sqrt{\frac{N}{2\pi\sigma^2}} \exp\left(-\frac{\rho^2}{4\sigma^2}\right) \exp(i\mathbf{k}_0 \cdot \boldsymbol{\rho}) . \quad (11)$$

To project the state onto the lattice eigenstate with Bloch wave vector \mathbf{k}_0 , one could switch on the optical lattice and allow the state (11) to evolve for a period of time. This would then transfer the condensate into the desired Bloch state. It should be noticed that this procedure for state preparation would work better for weak lattice potentials (and \mathbf{k}_0 a distance away from any energy gaps, of course). For strong lattice potentials the Gaussian state (11) may deviate enormously from the Bloch state \mathbf{k}_0 ; thus the projection procedure may result in an atom cloud with extremely low density. To overcome this difficulty, one may first project the state onto a weak-potential eigenstate and afterwards increase the lattice strength steadily.

In figure 3 we demonstrate manipulation of coherent atom waves utilizing the scheme proposed in the previous section. Here we start at $t = 0$ from the Gaussian wave packet (11) with $\sigma = 2.5a$, $N = 2\pi\sigma^2$, and $\mathbf{k}_0 = (\frac{\pi}{2a}, \frac{5\pi}{2a})$. The state is left to evolve in the optical lattice (2) with $V_0 = 1.0E_R$ for the period of time $\Delta t = 1.0T_B$. We then turn on the acceleration $g = \frac{\pi E_R}{4ma}$ along the $(1, 1)$ direction for the duration $\Delta t = 1.0T_B$, sending the state to the point $\mathbf{k} = (\frac{1+2\sqrt{2}}{2} \frac{\pi}{a}, \frac{5+2\sqrt{2}}{2} \frac{\pi}{a}) \simeq (\frac{1.914\pi}{a}, \frac{3.914\pi}{a})$,

and then switch it off. The condensate is then left to evolve in the lattice potential for another period of time $\Delta t = 2.0 T_B$. As one can see in figure 3, the condensate begins to split at $t = 2.0 T_B$ and two pulses of atom clouds become visible in the plot for $t = 3.0 T_B$. To further split the two pulses, at $t = 4.0 T_B$ we apply the acceleration $-\mathbf{g}$, which is opposite to that applied earlier. We turn off the acceleration after the duration $\Delta t = 1.0 T_B$ and allow the pulses to evolve in the lattice freely. The reverted acceleration brings the two pulses across the beam-splitting points $\mathbf{k} = (\pm \frac{\pi}{a}, \frac{3\pi}{a})$. Therefore, as shown in figure 3, at $t = 6.0 T_B$ each of the two pulses splits again into two further sub-pulses. All these results are consequences of the processes expounded in the previous section. One can see that by exploring Bragg reflection and Landau-Zener tunnelling of the condensate in accelerated 2D optical lattices, we have furnished a beam splitter that may be useful for manipulation of atom waves. By changing the lattice strength V_0 and/or the magnitude of the acceleration g , one can tune the relative strengths between the reflected and the transmitted pulses. Further manipulations of the atom cloud can be achieved by extensive exploration of the energy landscape for the optical lattice. For instance, one can apply \mathbf{g} in arbitrary directions, change \mathbf{g} in real time, and/or make use of different lattice structures (which may also involve “defects”). A simple example for the interference of coherent atom waves is shown in the plot for $t = 7.0 T_B$ in figure 3.

4. Conclusions and discussions

The interplay between cold atom physics and solid-state physics has stimulated exciting developments in the past decades. In this work, we have studied the dynamics of a cloud of ultracold atoms subject to an accelerated 2D optical square lattice by numerically solving the GP equation in the regime where mean-field interaction is negligible. We have shown that for sufficiently large accelerations the condensate can generate pulses of atom clouds that have structures richer than its 1D counterparts. Using a semiclassical picture, we have demonstrated that these structures can be understood from the \mathbf{k} -space dynamics of the Bloch state. In particular, Bragg reflection and Landau-Zener tunnelling at higher energy bands are shown to be responsible for the pattern generated.

On the one hand, our result can help envisage 2D atom lasers that have patterned output pulses. These patterns are closely connected with the underlying lattice structures. On the other hand, we have shown that by appropriately controlling the magnitude, direction, and duration of the lattice acceleration, one would be able to manipulate the atom wave by exploring the energy landscape of the optical lattice. We have demonstrated that a beam splitter for coherent atom waves can be furnished in this scheme.

An important issue that we did not address in this article is the effect of the nonlinear mean-field interaction in (1). Besides decoherence of the condensate as discussed in section 2.1 [12, 24], it has been shown that nonlinear effects can cause asymmetric Landau-Zener tunnelling and modulation instability for condensates in

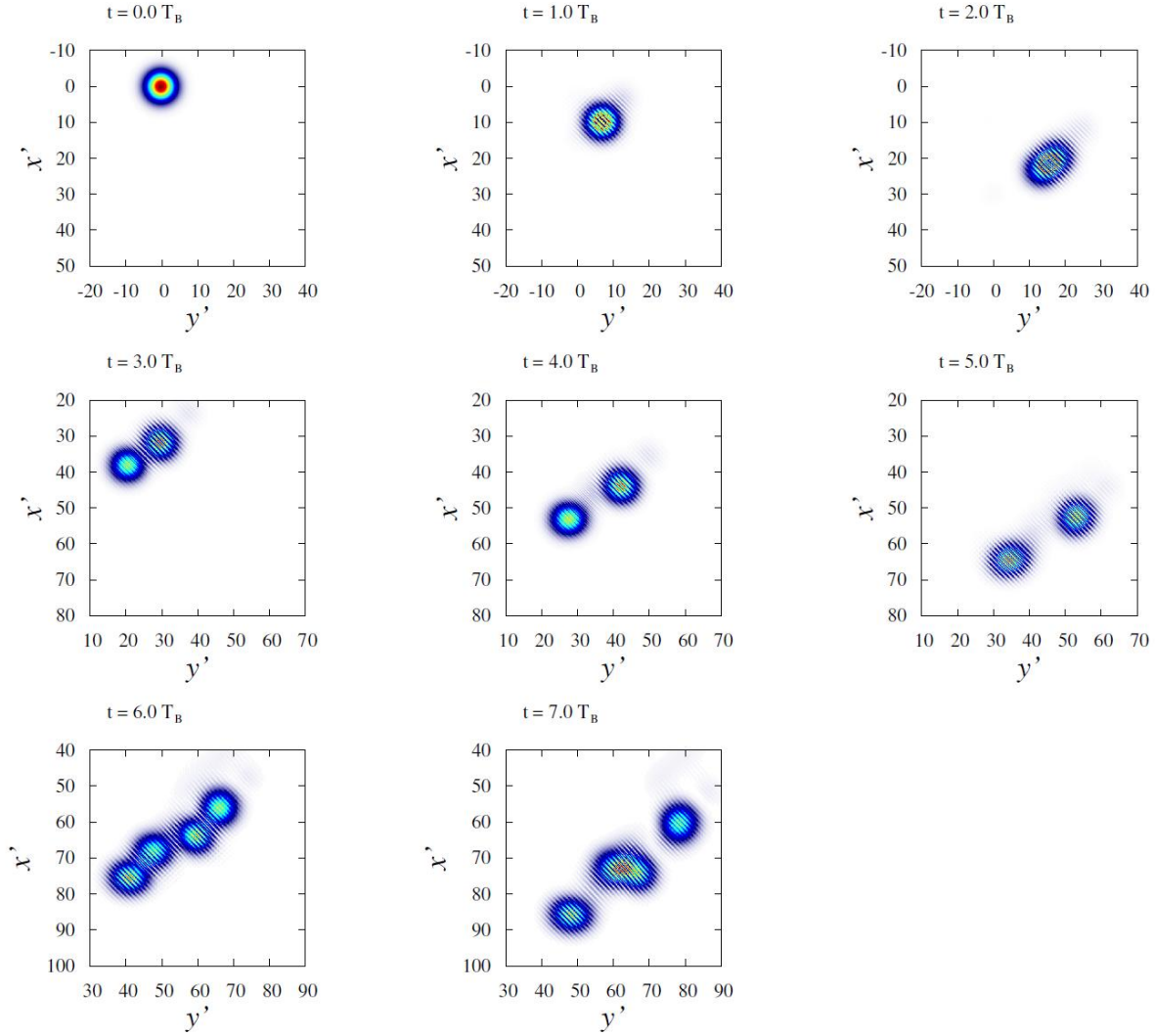


Figure 3. Numerical simulation for an accelerated condensate that starts from the initial wave function (11) with $\mathbf{k}_0 = (\frac{\pi}{2a}, \frac{5\pi}{2a})$ in the same 2D optical lattice as in figure 1. An acceleration $g = \frac{\pi}{4} \frac{E_B}{ma}$ is applied along the (1, 1) direction in a controlled manner as described in the text. As in figure 1 (b), here the time scale T_B is given by (7) and the plots are made against the rotated coordinates x' and y' in units of the lattice constant a . Notice that for different time frames we have shifted the coordinates to different ranges for convenience.

accelerated 2D optical lattices [20, 21]. We hope to investigate these problems in future publications. At the same time, possible applications ensue from this work in the fields of atom optics and quantum information sciences are also yet to be explored.

Acknowledgments

The authors would like to thank Profs. Sungkit Yip, Chung-Yu Mou, and Chien-Hua Pao for valuable discussions. This research was supported by NSC of Taiwan through

grant numbers NSC 96-2112-M-194-011-MY3, and NSC 98-2112-M-194-001-MY3; it is also partly supported by the Center for Theoretical Sciences, Taiwan.

References

- [1] Bloch I 2008 *Science* **319** 1202
- [2] Morsch O and Oberthaler M 2006 *Rev. Mod. Phys.* **78** 179
- [3] Ashcroft N W and Mermin N D 1976 *Solid State Physics* (Singapore: Thomson Learning)
- [4] Ziman J M 1972 *Principles of the Theory of Solids* 2nd ed (Cambridge: Cambridge University Press)
- [5] Raizen M, Salomon C and Niu Q 1997 *Phys. Today* **50**(7) 30
- [6] Pitaevskii L and Stringari S 2003 *Bose-Einstein Condensation* (Oxford: Oxford University Press)
- [7] Couvert A, Jeppesen M, Kawalec T, Reinaudi G, Mathevet R and Guéry-Odelin D 2008 *Europhys. Lett.* **83** 50001
- [8] Ben Dahan M, Peik E, Reichel J, Castin Y and Salomon C 1996 *Phys. Rev. Lett.* **76** 4508
- [9] Wilkinson S R, Bharucha C F, Madison K W, Niu Q and Raizen M G 1996 *Phys. Rev. Lett.* **76** 4512
- [10] Bharucha C F, Madison K W, Morrow P R, Wilkinson S R, Sundaram B and Raizen M G 1997 *Phys. Rev. A* **55** R857
- [11] Anderson B P and Kasevich M A 1998 *Science* **282** 1686
- [12] Anderson B P and Kasevich M A 1999 in *Proceedings of the International School of Physics “Enrico Fermi”, Course CXL* ed M Inguscio *et al* (Amsterdam: IOS Press) pp 439-452
- [13] Kolovsky A R and Korsch H J 2003 *Phys. Rev. A* **67** 063601
- [14] Witthaut D, Keck F, Korsch H J and Mossmann S 2004 *New J. Phys.* **6** 41
- [15] Breid B M, Witthaut D and Korsch H J 2007 *New J. Phys.* **9** 62
- [16] Trompeter H, Krolikowski W, Neshev D N, Desyatnikov A S, Sukhorukov A A, Kivshar Y S, Pertsch T, Peschel U and Lederer F 2006 *Phys. Rev. Lett.* **96** 053903
- [17] Shchesnovich V S, Cavalcanti S B, Hickmann J M and Kivshar Y S 2006 *Phys. Rev. E* **74** 056602
- [18] Shchesnovich V S, Desyatnikov A S and Kivshar Y S 2008 *Opt. Express* **16** 14076
- [19] Dreisow F, Szameit A, Heinrich M, Pertsch T, Nolte S and Tünnermann A 2009 *Phys. Rev. Lett.* **102** 076802
- [20] Brazhnyi V A, Konotop V V and Kuzmiak V 2006 *Phys. Rev. Lett.* **96** 150402
- [21] Brazhnyi V A, Konotop V V, Kuzmiak V and Shchesnovich V S 2007 *Phys. Rev. A* **76** 023608
- [22] Greiner M, Bloch I, Mandel O, Hänsch T W and Esslinger T 2001 *Phys. Rev. Lett.* **87** 160405
- [23] Jaksch D, Bruder C, Cirac, J I, Gardiner C W and Zoller P 1998 *Phys. Rev. Lett.* **81** 3108
- [24] Orzel C, Tuchman A K, Fenselau M L, Yasuda M and M A Kasevich 2001 *Science* **291** 2386
- [25] Greiner M, Mandel O, Esslinger T, Hänsch T W and Bloch I 2002 *Nature* **415** 39
- [26] Inouye S, Andrews M R, Stenger J, Miesner H-J, Stamper-Kurn D M and Ketterle W 1998 *Nature* **392** 151
- [27] Chin C, Grimm R, Julienne P and Tiesinga E 2010 *Rev. Mod. Phys.* **82** 1225
- [28] Hadzibabic Z, Stock S, Battelier B, Bretin V, and Dalibard J 2004 *Phys. Rev. Lett.* **93** 180403
- [29] Press W H, Teukolsky S A, Vetterling W T and Flannery B P 2002 *Numerical Recipes in C++: The Art of Scientific Computing* 2nd ed (Cambridge: Cambridge University Press)
- [30] Ting W C, Han D J and Wu S T 2010 Work in progress